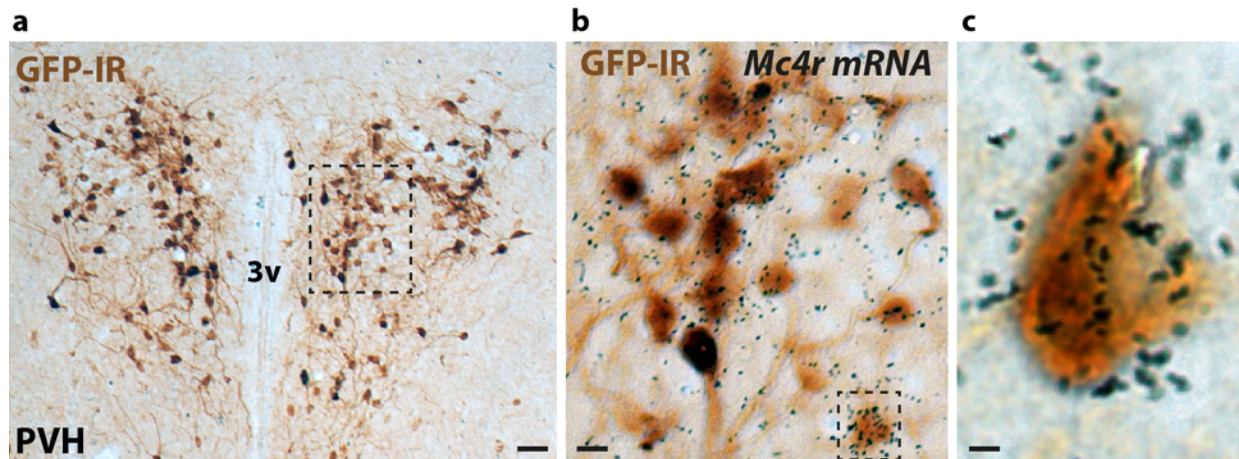


Supplementary Figure 1

Central *Mc4r-t2a-Cre* expression

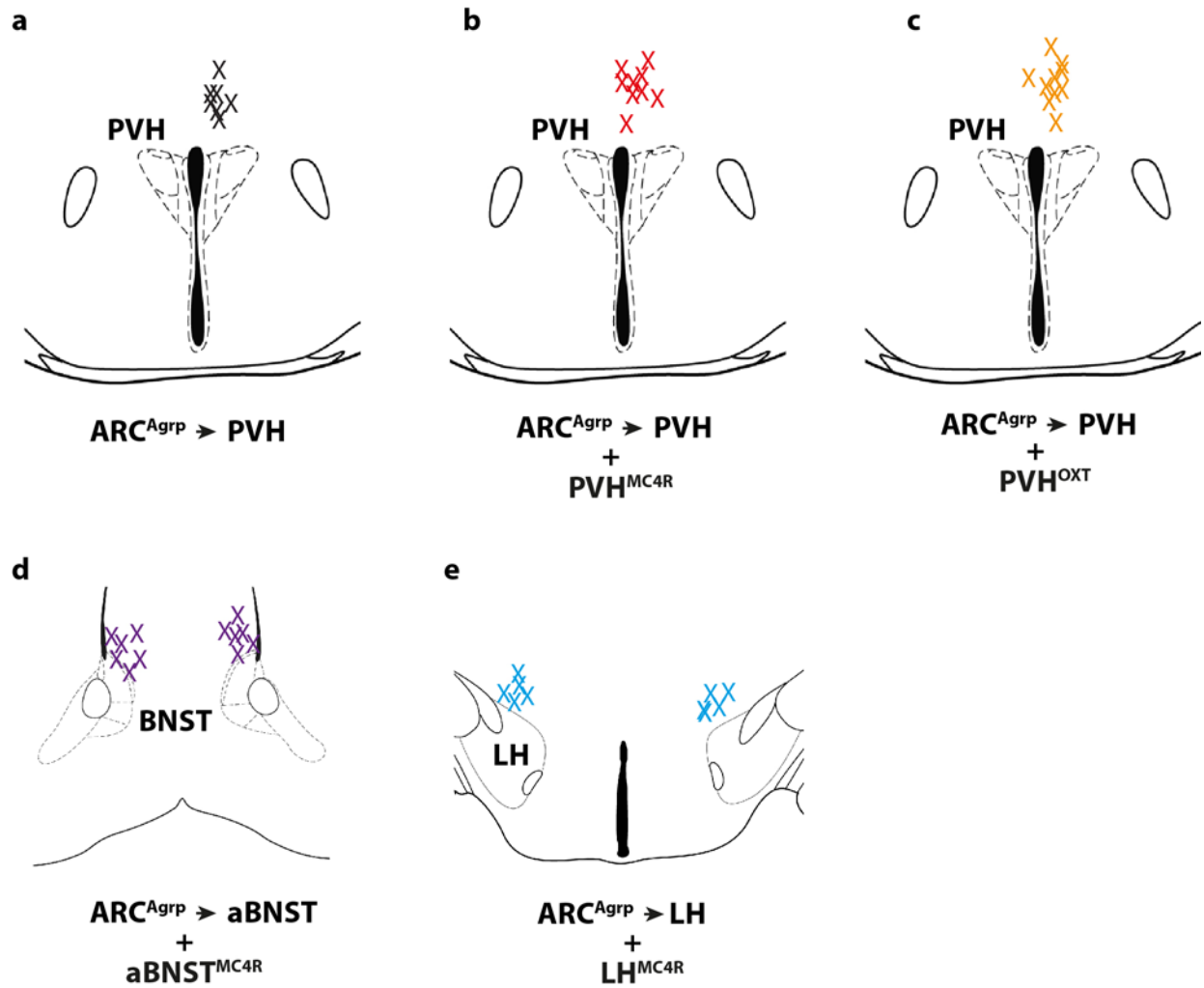
Mc4r-t2a-Cre expression was demarked by a germline *R26-loxSTOPlox-tdTomato* reporter allele and assayed across the rostral-caudal extent of the murine neuraxis. The neuroanatomical distribution of MC4R::tdTomato expressing neurons was consistent with the endogenous *Mc4r* expression profile. Abbreviations: BNST, bed nucleus of the stria terminalis; CeM, central amygdaloid nucleus; DMV, dorsomedial nucleus of the vagus; IML, intermediolateral nucleus; LH, lateral hypothalamus; LPBN, lateral parabrachial nucleus; NTS, nucleus of the solitary tract; PVH, paraventricular nucleus of the hypothalamus; VMH, ventromedial nucleus of the hypothalamus. Scale bar = 100 μ m.



Supplementary Figure 2

Validation of PVH *Mc4r-t2a-Cre* expression

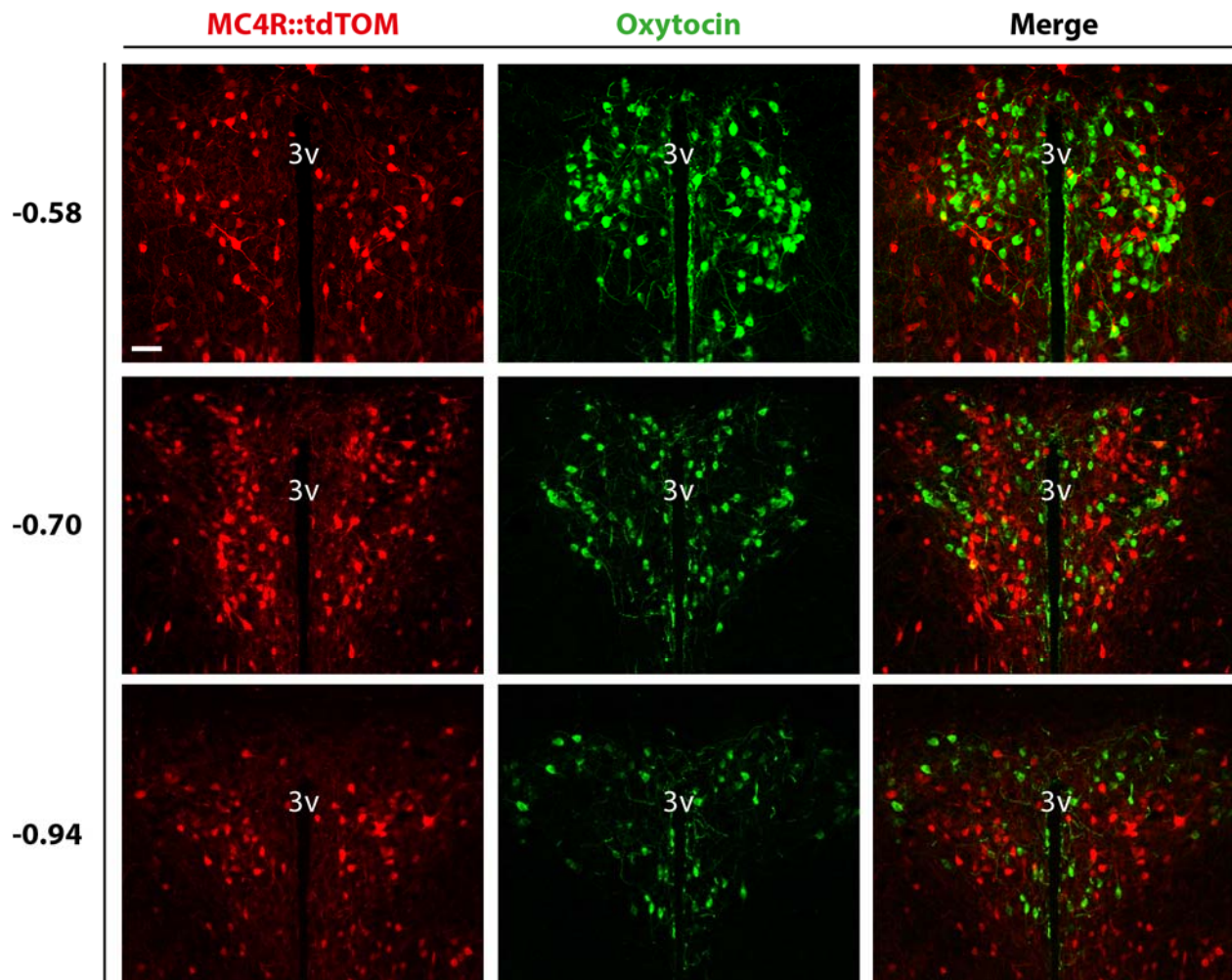
Mc4r-t2a-Cre expression within the paraventricular nucleus of the hypothalamus (PVH) was demarked by injection of a cre-dependent AAV8-hSyn-DIO-GFP viral construct. Colocalization of *Mc4r-t2a-Cre::GFP* expression with endogenous *Mc4r* mRNA was determined by way of dual immunohistochemistry (for GFP, brown soma) and radioactive in situ hybridization (for *Mc4R* mRNA, black puncta). Microscopic analysis revealed extensive colocalisation of the two signals. a, scale bar = 500 μ m; b, scale bar = 50 μ m; c, scale bar = 10 μ m.



Supplementary Figure 3

Neuroanatomical location of optic fibers for *in vivo* optogenetic occlusion studies

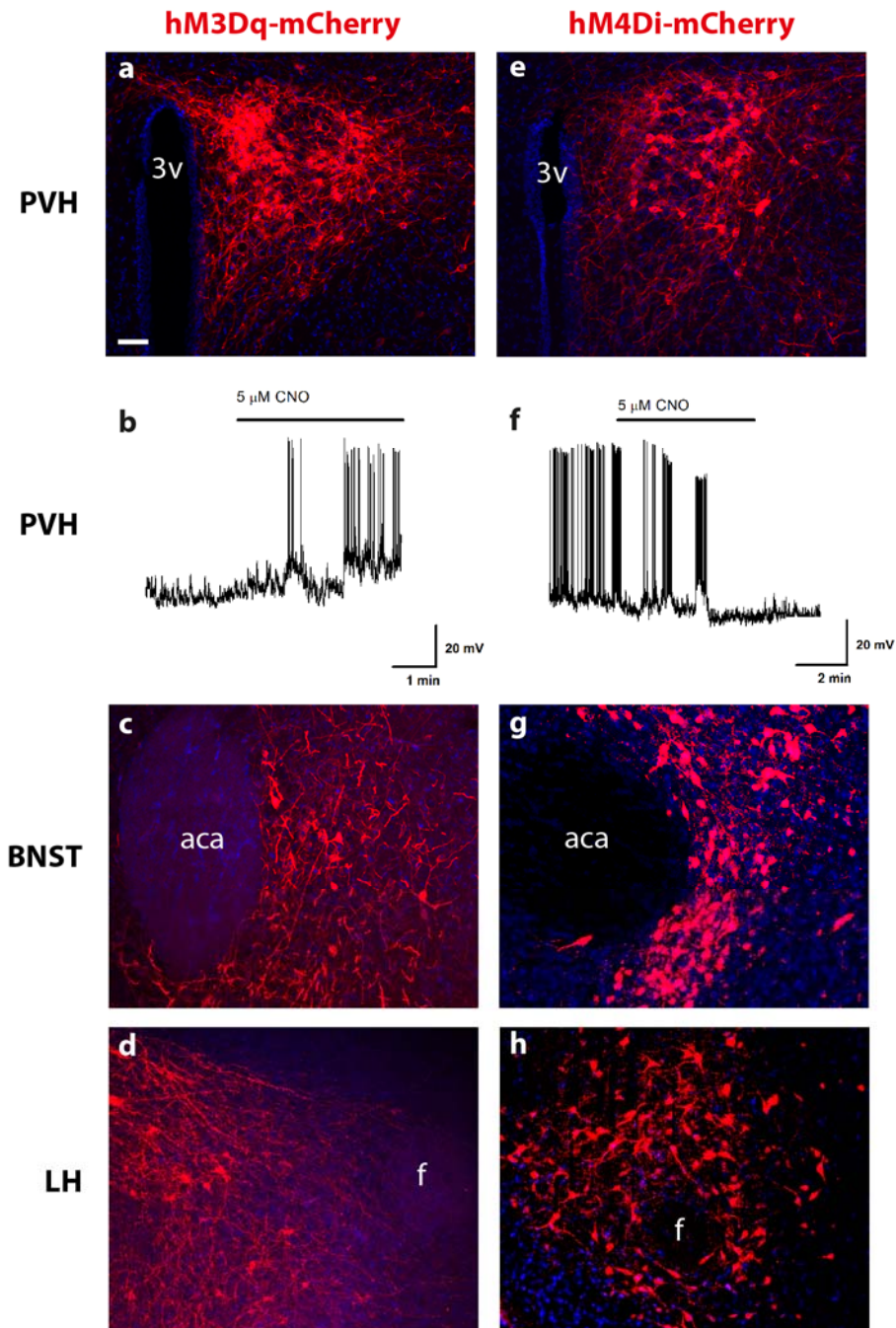
Mice used for optogenetic occlusion studies were validated for fiber placement using histological sections. The approximate positions of the fibers is denoted by an X. **a-c**, Relates to Figure 1g-h. **d**, Relates to Figure 2d. **e**, Relates to Figure 2e. Abbreviations: BNST, bed nucleus of the stria terminalis; LH, lateral hypothalamus; LPBN, lateral parabrachial nucleus; PVH, paraventricular nucleus of the hypothalamus.



Supplementary Figure 4

PVH^{MC4R} neurons do not express oxytocin

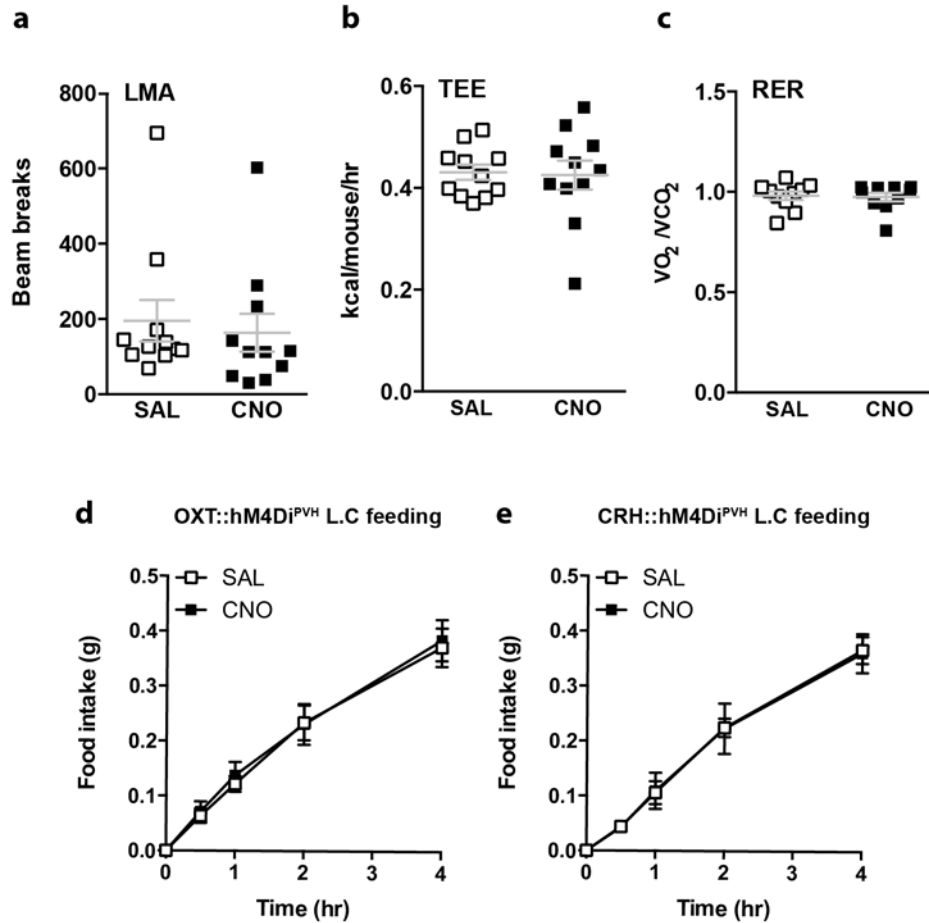
Fluorescent immunohistological analysis of *MC4R-t2a-Cre::tdTomato* (red) and endogenous oxytocin (green) expression in the PVH revealed the complete absence of colocalization at all neuroanatomical levels. Abbreviations: 3v, third ventricle. Scale bar = 100 μ m.



Supplementary Figure 5

Validation of *in vivo* DREADD expression and function

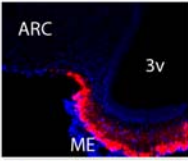

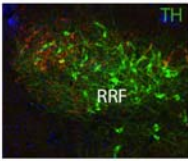
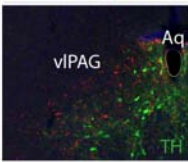
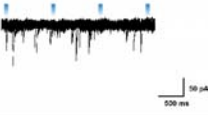
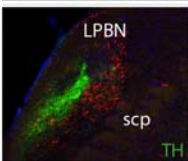
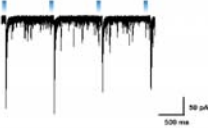
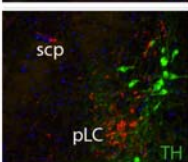
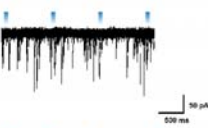
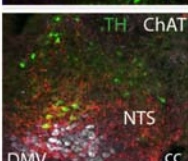
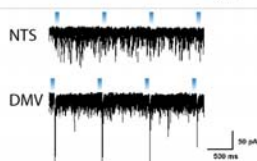
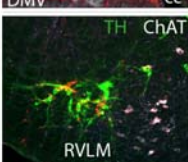
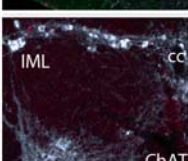
a-d, Validation of excitatory hM3Dq-mCherry expression in *Mc4r-t2a-Cre* mice. **a**, Representative image of hM3Dq-mCherry expression within the PVH. **b**, Membrane potential and firing rate of *Mc4r-t2a-Cre::hM3Dq-mCherry*^{PVH} neurons increased upon 5 μM CNO application during electrophysiological current clamp recordings. **c**, Representative image of hM3Dq-mCherry expression within the BNST. **d**, Representative image of hM3Dq-mCherry expression within the LH. **e-h**, Validation of inhibitory hM4Di-mCherry expression in *Mc4r-t2a-Cre* mice. **e**, Representative image of hM4Di-mCherry expression within the PVH. **f**, Membrane potential and firing rate of *Mc4r-t2a-Cre::hM4Di-mCherry*^{PVH} neurons decreased upon 5 μM CNO application electrophysiological current clamp recordings. **g**, Representative image of hM4Di-mCherry expression within the BNST. **h**, Representative image of hM4Di-mCherry expression within the LH. Abbreviations: 3v, third ventricle; aca, anterior commissure anterior part; f, fornix. Scale bar in **a**, = 100 μm and relates to all images.



Supplementary Figure 6

PVH^{MC4R} neurons do not influence energy expenditure or locomotor activity, while either PVH^{OXT} or PVH^{CRH} neurons do not influence food intake

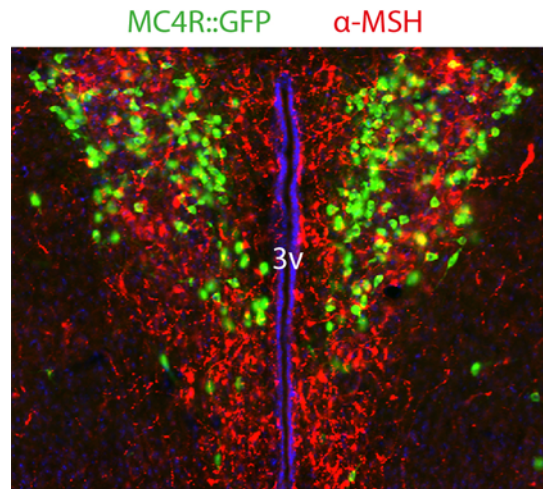
a-c, Chemogenetic activation of PVH^{MC4R} neurons did not influence **a**, locomotor activity (LMA; $n=11$, Paired two-tailed t-test, $t_{(10)}=0.43$, $p=0.67$), **b**, total energy expenditure (TEE; $n=11$, Paired two-tailed t-test, $t_{(10)}=0.20$, $p=0.85$) or **c**, respiratory exchange ratio (RER; $n=11$, Paired two-tailed t-test, $t_{(10)}=0.35$, $p=0.79$). **d-e**, PVH^{OXT} and PVH^{CRH} neurons do not influence feeding behavior. **d**, Chemogenetic inhibition of PVH^{OXT} neurons did not significantly affect light-cycle food intake, compared to the same mice treated with saline ($n=6$, Repeated measures ANOVA, main effect of treatment and interaction not significant, main effect of time ($F_{(4,25)}=70.31$, $p<0.0001$)). **e**, Chemogenetic inhibition of PVH^{CRH} neurons did not significantly affect light-cycle food intake, compared to the same mice treated with saline ($n=5$, Repeated measures ANOVA, main effect of interaction and treatment not significant, main effect of time ($F_{(3,16)}=20.61$, $p<0.0001$)).

	Syn-mCherry	Relative density	CRACM	Response	% connected
ME		ARC: - ME: +++		ARC ^{AgRP} 10/10	0%
RRF		+	-	-	-
vIPAG		++		28/30	7%
LPBN		+++		11/19	56%
pLC		+		10/10	0%
NTS DMV		NTS: +++ DMV: +++		NTS: 37/39 DMV: 11/20	5% 55%
RVLM		+	-	-	-
IML		+	-	-	-

Supplementary Figure 7

Efferent targets and connectivity of PVH^{MC4R} projections

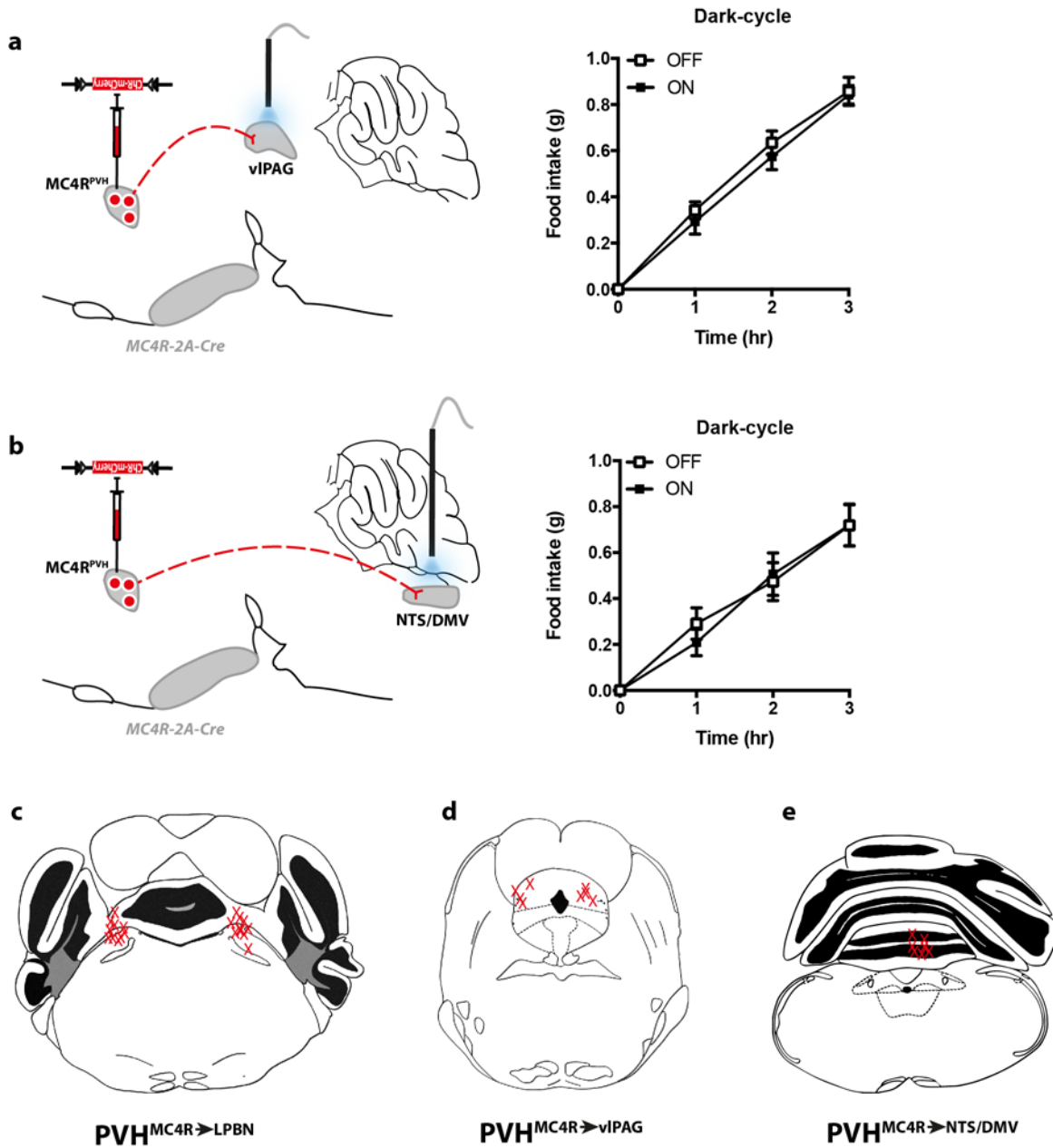
Neuroanatomical projection mapping from PVH^{MC4R} neurons was achieved via unilateral stereotaxic injection of a synaptically targeted fluorophore (AAV8-hSyn-FLEX-Syn-mCherry). PVH^{MC4R} neurons exhibit exclusively descending and predominantly ipsilateral projections to the median eminence (ME), retrorubral field (RRF), ventrolateral periaqueductal grey (vIPAG), lateral parabrachial nucleus (LPBN), pre-locus coeruleus (pLC), nucleus of the solitary tract (NTS), dorsal motor nucleus of the vagus (DMV), rostral ventrolateral medulla (RVLM) and intermediolateral nucleus (IML). Qualitative assessment of fiber density demonstrated that the ME, LPBN and NTS received the densest innervation. CRACM analysis: No light-evoked EPSCs were detected on ARC^{AgRP} neurons, confirming the uni-directionality of the ARC^{AgRP}→PVH^{MC4R} circuit. The vIPAG, pLC and NTS exhibited low to no connectivity, 7%, 0% and 5%, respectively. 56% of LPBN and 55% of DMV of randomly patched post-synaptic neurons exhibited light-evoked EPSCs. Abbreviations: 3v, third ventricle; Aq, aqueduct; cc, central canal; ChAT, choline acetyltransferase; scp, superior cerebellar peduncle; TH, tyrosine hydroxylase.



Supplementary Figure 8

PVH^{MC4R} neurons lie within the ARC^{POMC}→PVH efferent field

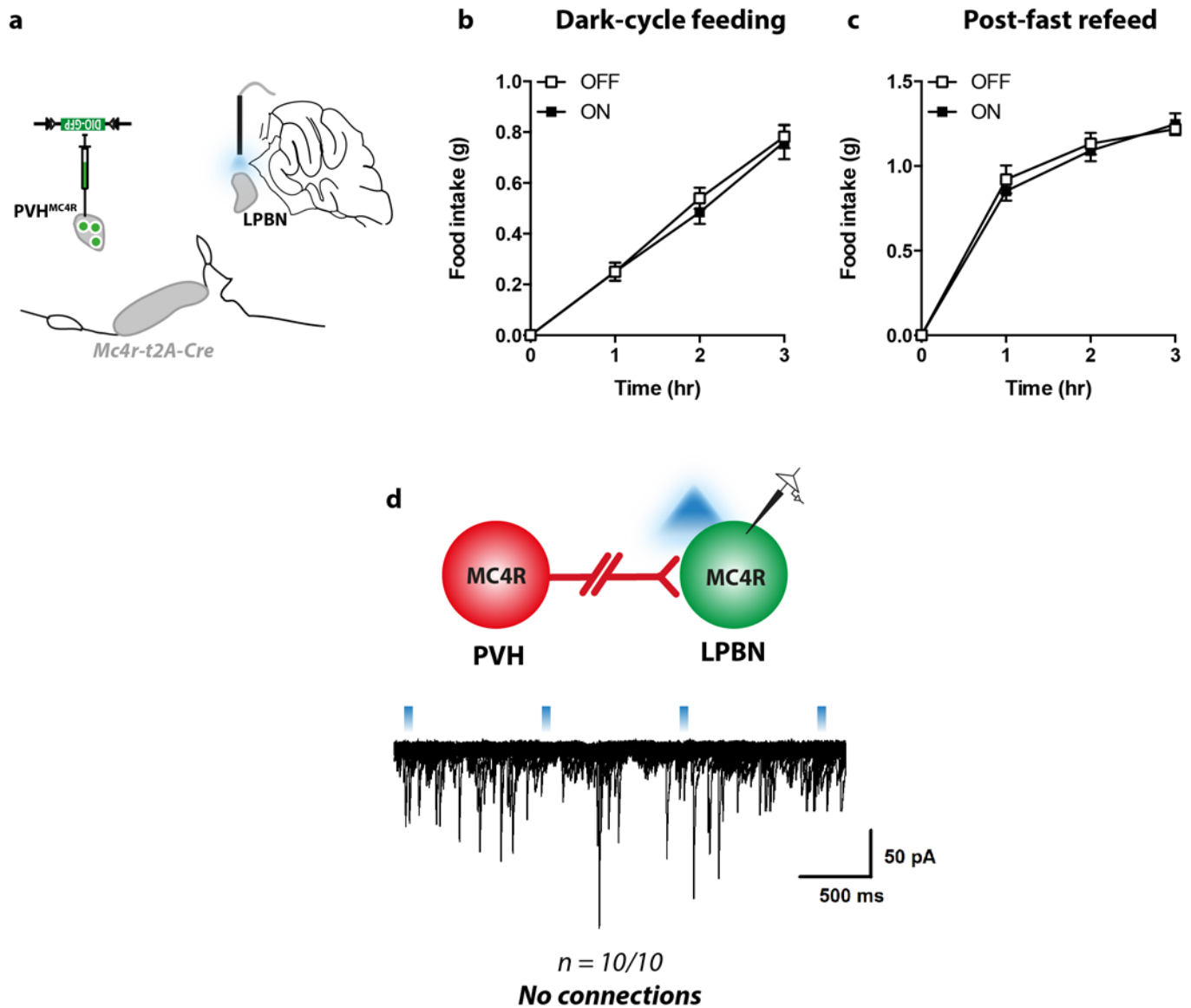
Fluorescent immunohistological analysis of *MC4R-t2a-Cre::R26-loxSTOPlox-L10-GFP* (green) and endogenous alpha-melanocyte-stimulating hormone (red) expression in the PVH revealed these two fields to be overlapping. Abbreviations: 3v, third ventricle. Scale bar = 100 μm.



Supplementary Figure 9

PVH^{MC4R}→vIPAG or PVH^{MC4R}→NTS/DMV neurons do not influence feeding behavior

a-b, *in vivo* optogenetic stimulation of PVH^{MC4R}→vIPAG (a; n=4, Repeated measures ANOVA, main effect of interaction and treatment not significant, main effect of time ($F_{(3,12)}=76.00$, $p<0.0001$) and PVH^{MC4R}→NTS/DMV (b; n=5, Repeated measures ANOVA, main effect of interaction and treatment not significant, main effect of time ($F_{(3,16)}=20.61$, $p<0.0001$) terminals does not promote satiety during dark-cycle feeding. **c-e**, PVH^{MC4R}→LPBN (c), PVH^{MC4R}→vIPAG (d), PVH^{MC4R}→NTS/DMV (e) mice used for optogenetic feeding and RTPP studies were validated for fiber placement using histological sections. The approximate positions of the fibers is denoted by an X.



Supplementary Figure 10

PVH^{MC4R} → LPBN photostimulation in the absence of ChR2-mCherry does not influence food intake

a, PVH^{MC4R} neurons were transduced with cre-dependent GFP and optic fibers placed bilaterally over the LPBN. **b**, Photostimulation of PVH^{MC4R}::GFP LPBN terminals had no effect on food intake during the dark-cycle, compared to the same mice without photostimulation (*n*=10, Repeated measures ANOVA, main effect of treatment and interaction not significant, main effect of time ($F_{(3,36)}=95.38$, $p<0.0001$). **c**, following an overnight fast, as compared to same mice without photostimulation (*n*=10, Repeated measures ANOVA, main effect of treatment and interaction not significant, main effect of time ($n=6$, $F_{(3,20)}=132.6$, $p<0.0001$). **d**, PVH^{MC4R} neurons do not make synaptic contact with LPBN^{MC4R} neurons. Channelrhodopsin-assisted circuit mapping between pre-synaptic PVH^{MC4R} neurons (red) and putative post-synaptic LPBN^{MC4R} neurons (green) in an *Mc4r-t2a-Cre::R26-loxSTOPlox-L10-GFP* mouse line revealed the absence of light-evoked EPSCs in all cells tested.

#